the polymerizability of a given monomer system. In particular, we have shown how electronic rather than steric factors are crucial in this regard for the systems considered here. Further, these new polymers bearing a fluorophoric functionality may represent a useful addition to the array of functionalized conducting polymers previously reported.[1-29]

Acknowledgment. This work was supported in part by the Defense Advanced Research Projects Agency (contract monitored by the Office of Naval Research) and by the Robert A. Welch Foundation (Grant Y-743). It is also a pleasure to thank Drs. E. W. Tsai and V. D. Panchalingam for contributions to the voltammetric and NMR experiments.

Anodic Electrosynthesis of CdTe Thin Films

Dong Ham, Kamal K. Mishra, Alex Weiss,† and Krishnan Rajeshwar*

Department of Chemistry, The University of Texas at Arlington, Arlington, Texas 76019

Received July 10, 1989

Cadmium telluride thin films were anodically electrosynthesized by using Cd anodes in an alkaline solution of sodium telluride. Thermodynamic (Pourbaix) analyses predicted that the oxidation of Te^{2-} to CdTe was more favorable relative to the corresponding $Te^{2-} \rightarrow Te^0$ reaction. Hydrodynamic and cyclic voltammetry permitted detailed characterization of the Cd and Te electrochemistry in alkaline media. Cyclic photovoltammetry, wherein a Cd anode was intermittently illuminated with white light during potential cycling, unequivocally showed the formation of a photoelectrochemically responsive n-type CdTe thin film atop the Cd substrate surface. These films were also formed *at open circuit* via an electroless route. The CdTe thin films thus formed were further characterized by their photoaction spectra in alkaline Te^{2-}/Te_2^{2-} electrolyte and by surface analyses including Auger and X-ray photoelectron spectroscopy, scanning electron microscopy, and scanning Auger microscopy. The virtue of the anodic electrosynthesis route in terms of avoiding contamination of CdTe with Te^0 was clearly seen in these surface analysis data, especially when the corresponding results obtained for the cathodically synthesized thin films in these laboratories and elsewhere were compared.

Introduction

Cadmium telluride is an attractive compound semiconductor candidate for many optoelectronic applications.[1] Thin films of this material have been synthesized by a variety of techniques including vacuum evaporation, sputtering, close-spaced vapor transport, screen printing, spray pyrolysis, and chemical vapor deposition.[2] We[3-6] and others[7-10] have described the advantages of electrochemical syntheses in applications (e.g., solar, switching) wherein thin films with large electro- and photoactive areas are required. In these studies, a cathodic technique involving the codeposition of Cd^{2+} and $HTeO_2^+$ (or molecular Te in the case of nonaqueous media; cf. ref 11) was utilized. In principle, an anodic route ought to be possible involving a Cd anode and oxidizable Te^{2-} species in alkaline media. However, we are not aware of any successful attempts in the case of CdTe, although anodic techniques have been previously utilized for the synthesis of CdS,[12-17] PbS,[18,19] HgS,[20] and Bi_2S_3[12,13,21,22] thin films. We describe in this paper the electrodeposition chemistry and characterizaton of anodically electrosynthesized CdTe thin films. Thermodynamic (Pourbaix) analyses, cyclic and hydrodynamic voltammetry, cyclic photovoltammetry,[23] photoelectrochemical, and surface analyses are described for these thin films.

The second important finding in this work is an anodic *electroless* route to the synthesis of n-CdTe thin films, i.e., formation of n-type CdTe when a Cd anode is held at open circuit in an alkaline Te^{2-} solution. We will show how fairly stoichiometric CdTe may be electrosynthesized in this manner without admixture with Te as a separate phase

Table I. Glossary of Important Electrochemical Reactions in the Anodic Cd–Te System

	reaction	potential, V vs SCE
(1a)	$CdO + 2H^+ + 2e^- = Cd + H_2O$	−1.02
(1b)	$Cd(OH)_2 + 2e^- = Cd + 2OH^-$	−1.06
(2)	$HCdO_2^- + 3H^+ + 2e^- = Cd + 2H_2O$	0.58
(3)	$Te_2^{2-} + 2e^- = 2Te^{2-}$	−1.68
(4)	$Te + 2e^- = Te^{2-}$	−1.38
(5)	$2Te + 2e^- = Te_2^{2-}$	−1.06
(6)	$TeO_3^{2-} + 3H_2O + 4e^- = Te + 6OH^-$	−0.82
(7)	$TeO_4^{2-} + H_2O + 2e^- = TeO_3^{2-} + 2OH^-$	−0.33
(8)	$2TeO_3^{2-} + 12H^+ + 10e^- = Te_2^{2-} + 6H_2O$	0.25
(9)	$TeO_3^{2-} + 3H_2O + 6e^- = Te^{2-} + 6OH^-$	−1.04
(10)	$CdTe + 2e^- = Te^{2-} + Cd$	−1.86

† Department of Physics.

* Author to whom correspondence should be addressed.

(1) Zanio, K. *Semiconductors and Semimetals*; Academic Press: New York, 1978; Vol. 13.
(2) For example: *Proceedings of the IEEE Photovoltaic Specialists' Conference*; IEEE, New York.
(3) Bhattacharya, R. N.; Rajeshwar, K.; Noufi, R. N. *J. Electrochem. Soc.* **1984**, *131*, 939.
(4) Bhattacharya, R. N.; Rajeshwar, K. *J. Electrochem. Soc.* **1984**, *131*, 2032.
(5) Bhattacharya, R. N.; Rajeshwar, K.; Noufi, R. N. *J. Electrochem. Soc.* **1985**, *132*, 732.
(6) Bhattacharya, R. N.; Rajeswar, K. *J. Appl. Phys.* **1985**, *58*, 3590.
(7) Panicker, M. P. R.; Knaster, M.; Kröger, F. A. *J. Electrochem. Soc.* **1978**, *125*, 566.
(8) Fulap, G.; Doty, M.; Meyers, P.; Betz, J.; Liu, C. H. *Appl. Phys. Lett.* **1982**, *40*, 327.
(9) Tukahashi, M.; Uosaki, K.; Kita, H.; Yamaguchi, S. *J. Appl. Phys.* **1986**, *60*, 2046.
(10) Basol, B. M. *Solar Cells* **1988**, *23*, 69.

0897-4756/89/2801-0619$01.50/0

(a common problem with the synthesis of CdTe; cf. ref 24). This is feasible because of the fortuitous location of the open-circuit potential of Cd anodes in the Te^{2-} electrolyte which lies negative of the $Te^{2-/0}$ redox point. (Table I contains a glossary of important electrochemical reactions in the Cd-Te system.) We had previously shown[3] how CdTe thin films could be electrosynthesized via a *cathodic* electroless route; the material in this case, however, was p-type.

Experimental Section

Electrochemistry/Photoelectrochemistry. A standard single-compartment three-electrode electrochemical cell was used in all the cases; the reference electrode was saturated calomel/1 M KCl (SCE), and a Pt spiral was utilized as the counter electrode. All potentials below are quoted with respect to SCE reference. The working electrodes were either glassy carbon (GC) in disk form or cadmium in both disk and foil forms. An EG&G Princeton Applied Research Model 273 electrochemistry system was used in conjunction with a Houston Instrument Model 2000 *X–Y* recorder.

The instrumentation for cyclic photovoltammetry (CPV) has been previously described.[23,25] Briefly, this technique consists of examining the current response of the electrodeposit/electrolyte interphase under conditions of voltammetric scanning and modulated light excitation. Thus, the photoresponse of the forming semiconductor serves as an in situ diagnostic probe of the deposition mechanism. For example, if the forming semiconductor were n-type and when potentials positive of its flatband location are accessed, a modulated anodic photocurrent flow should be observed that is superimposed on the nominal dark current envelope. An ELH tungsten halogen lamp was used as a white light source for CPV; a nominal light intensity of 100 mW/cm^2 (not corrected for reflection/absorption losses in the cell/electrolyte) was used in these experiments. Photoaction spectra were obtained with a minicomputer-controlled Spectrodata SD 90 system comprising a quartz tungsten halogen lamp assembly (Model 40-130) and an Ebert 250-mm monochromator (Monospec 25, Model 82-415). The photocurrents were measured in some cases (cf. Figure 6a) with an EG&G Model 5208 lock-in amplifier operated in conjunction with an EG&G Model 194A chopper.

Hydrodynamic voltammetry utilized a Pine Instrument Model RDE 4 bipotentiostat, an AFMSRX rotor, and a rotating-ring disk electrode (RRDE) assembly consisting of a GC disk and a Pt ring. The theoretical collection efficiency of 16.9% (r_1 = 0.256 cm, r_2 = 0.334 cm) was rechecked with calibration experiments using a $Fe(CN)_6^{3-/4-}$ redox couple.

Chemicals. Solutions containing Te^{2-} ions were prepared by using a literature procedure.[26] A Te cathode was electrochemically reduced under a N_2 blanket in 1 M NaOH to generate Te_2^{2-} (reaction 5, Table I). These ditelluride anions were further reduced chemically by the addition of sodium dithionite to the electrolyte at ~60–70 °C. This reduction could be conveniently monitored and was facile as signalled by rapid color change from purple (Te_2^{2-}) to colorless (Te^{2-}):

$$2Te + 2e^- = Te_2^{2-} \quad (5)$$

$$3Te_2^{2-} + 6e^- = 6Te^{2-} \quad (3)$$

$$S_2O_4^{2-} + 4OH^- = 2SO_4^{2-} + 4H^+ + 6e^- \quad (11)$$

All the electrochemical and photoelectrochemical measurements described in this paper pertain to 1 M NaOH electrolyte under a N_2 blanket.

Surface Analyses. Surface analyses including X-ray photoelectron spectroscopy (XPS), Auger electron spectroscopy (AES), scanning electron microscopy (SEM), and scanning Auger microscopy (SAM) were performed on a Perkin-Elmer 560 (PE 560) electron spectrometer. Auger depth profiling was accomplished by sputtering using 2-keV krypton ions. The sputter rate was calibrated on a ZnS sample of known thickness to be ~100 Å/min. An Al anode was used in the XPS measurements. The high-resolution scans were performed with a spectrometer pass energy of 50 eV.

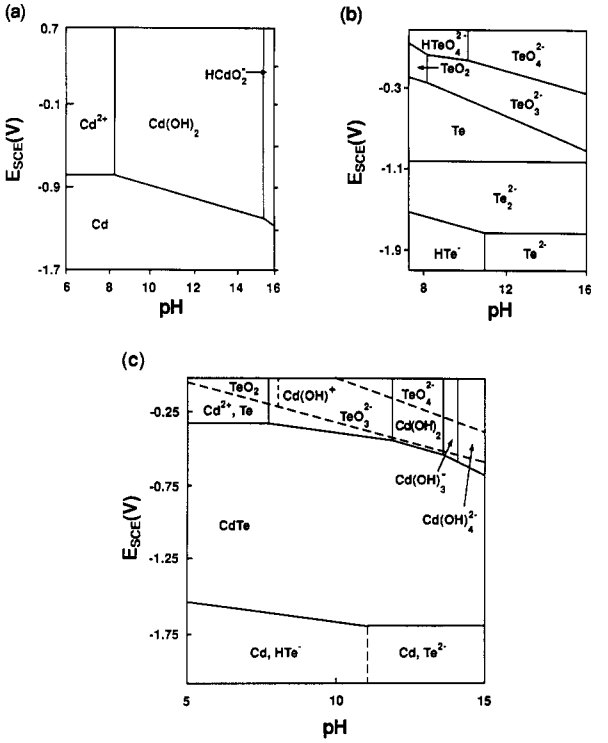

Figure 1. Pourbaix diagrams for (a) Cd–H_2O, (b) Te–H_2O, and (c) Cd–Te–H_2O systems. Only the partial diagrams are shown, and the representation in part c is adapted from ref 28. Other data are from ref 27.

Results and Discussion

Thermodynamic Considerations. Figure 1 contains partial Pourbaix (*E*–pH) diagrams for the Cd–H_2O, Te–H_2O, and Cd–Te–H_2O systems at 25 °C. In these analyses, the activity of the dissolved species (a_{Cd}, a_{Te}) has been taken to be 0.001. These diagrams have been adapted from the fuller versions in the literature (ref 27 and 28). As indicated by Figure 1a, Cd in high-pH media corrodes to form $Cd(OH)_2$; at extreme pH (>14), $HCdO_2^-$ is also thermodynamically stable. These corrosion processes are represented by reactions 1 and 2 in Table I.

Figure 1b predicts that at alkaline pH, Te^{2-} undergoes stepwise oxidation to Te_2^{2-}, Te, TeO_3^{2-}, and finally, TeO_4^{2-} (reactions 3–9 in Table I). It should be noted that these reactions are catalyzed by adventitious O_2, hence the need to maintain an inert atmosphere (cf. Experimental Sec-

(11) Baranski, A.; Bennett, M. S.; Fawcett, W. R. *J. Appl. Phys.* **1983**, *54*, 6390.
(12) Miller, B.; Heller, A. *Nature* **1976**, *262*, 680.
(13) Miller, B.; Menezes, S.; Heller, A. *J. Electroanal. Chem.* **1978**, *94*, 85.
(14) Peter, L. M. *Electrochim. Acta* **1978**, *23*, 165.
(15) Peter, L. M. *J. Electroanal. Chem.* **1979**, *98*, 49.
(16) Da Silva Pereira, M. I.; Peter, L. M. *J. Electroanal. Chem.* **1982**, *140*, 103.
(17) Yeh, L.-S. R.; Hudson, P. G.; Damjanovic, A. *J. Appl. Electrochem.* **1982**, *12*, 153.
(18) Scharifker, B.; Ferreira, Z.; Mozota, J. *Electrochim. Acta* **1985**, *30*, 677.
(19) Totland, K. M.; Harrington, D. A. *J. Electroanal. Chem.*, in press.
(20) Peter, L. M.; Reid, J. D.; Scharifker, B. R. *J. Electroanal. Chem.* **1981**, *119*, 73.
(21) Peter, L. M. *J. Electroanal. Chem.* **1979**, *98*, 59.
(22) Peter, L. M.; Wright, G. A. *Electrochim. Acta* **1987**, *32*, 1353.
(23) Mishra, K. K.; Rajeshwar, K. *J. Electroanal. Chem.*, in press.
(24) For example: Shin, S. H.; Bajaj, J.; Moudy, L. A.; Cheung, D. T. *Appl. Phys. Lett.* **1983**, *43*, 68.
(25) Mishra, K. K.; Rajeshwar, K. *J. Electroanal. Chem.*, in press.
(26) Ellis, A.; Kaiser, S. N.; Bolts, J. M.; Wrighton, M. S. *J. Am. Chem. Soc.* **1977**, *119*, 2839.

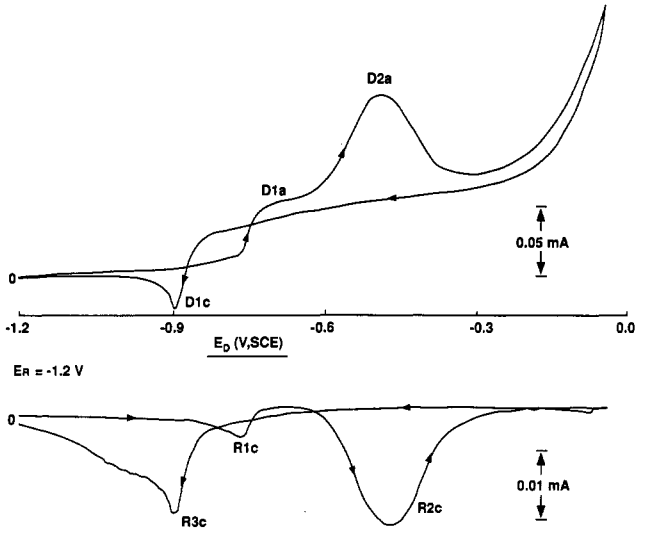

Figure 2. RRDE (GC disk, Pt ring) voltammograms for Te^{2-} oxidation in 1 M NaOH. The electrolyte contained 0.01 M Te^{2-}, and the disk was rotated at 400 rpm. The ring was held at −1.20 V vs SCE. The potential scan rate was 0.01 V s^{-1}.

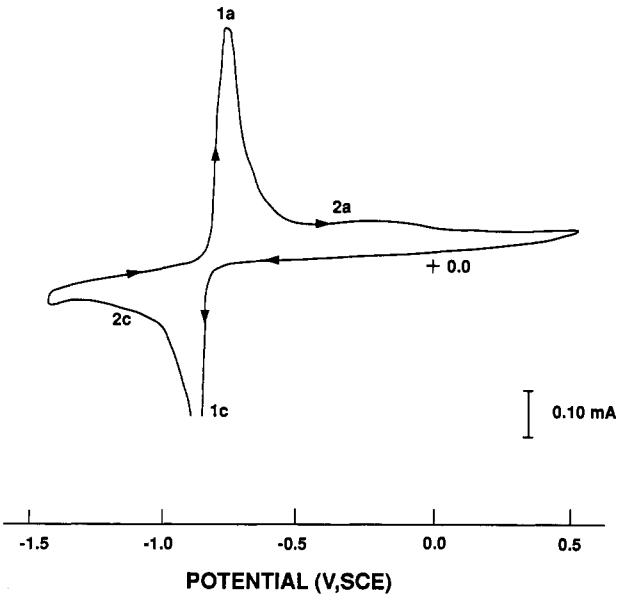

Figure 3. Cyclic voltammogram (potential scan rate 0.100 V s^{-1}) for a Cd risk in 1 M NaOH.

tion). A further complication with the Te–H_2O chemistry is disproportionation with the concurrent evolution of H_2.[27]

$$Te_2^{2-} = 2Te + 2e^- \quad (5)$$

$$Te_2^{2-} = Te + Te^{2-} \quad (12)$$

$$2H^+ + 2e^- = H_2 \quad (13)$$

As the Cd–Te–H_2O diagram in Figure 1c shows, the $CdTe/Te^{2-}$ boundary lies below the Te/Te^{2-} or Te_2^{2-}/Te^{2-} line, indicating that Te^{2-} can be oxidized at potentials negative of the free-element deposition; i.e., the interaction of Te^{2-} with Cd to form CdTe (reaction 10, Table I) is thermodynamically preferred to either reaction 4 or 5 in Table I. An alternative way of picturing the situation is that it is easier to oxidize Te^{2-} to CdTe (relative to formation of Te^0 as a separate phase) because of the reduction in a_{Te} within the film as a result of compound formation.[29] Figure 1c also predicts that anodic oxidation of CdTe leads to $Cd(OH)_2$ and TeO_3^{2-} in alkaline media.

Electrochemical Behavior. A brief discussion of Te electrochemistry in basic media is first presented as a prelude to the more complex Cd–Te–H_2O case. A more detailed study will be described elsewhere.[30] We also note in this context the early polarography studies of Lingane[31] and Panson[32] as well as more recent studies by other authors.[33,34]

Figure 2 contains representative RRDE data for 10^{-2} M Te in 1 M NaOH. The ring potential was held at −1.20 V to collect Te_2^{2-} ions generated at the disk via reaction 5;[30] the disk potential scan was initiated at −1.20 V in the positive direction. The mass-transfer-limited[30] current plateau labeled D1a is assigned to the oxidation of Te^{2-} to Te^0 (reaction 4, Table I). Some solubility of Te^0 in the electrolyte or the intermediate generation of Te_2^{2-} is implied by the correlated cathodic feature at the ring labeled R1c. Further anodic polarization of the disk results in a peak D2a with a correlated ring response, R2c. Interestingly enough, the ring collection efficiency for the species generated at the disk at this wave was ~1.2 times the theoretical value. We propose that D2a is associated with reaction 6 in Table I:

$$Te + 6OH^- = TeO_3^{2-} + 3H_2O + 4e^- \quad (6)$$

The corresponding reduction of TeO_3^{2-} to a more highly reduced form than Te at the ring will have to be invoked to account for the anomalous collection efficiency value. We suggest reaction 14:

$$TeO_3^{2-} + 6H^+ + 6e^- = Te^{2-} + 3H_2O \quad (14)$$

This $6e^-$ process at the ring (which has a literature precedent, cf. ref 33) vs the $4e^-$ reaction at the disk would rationalize the observed collection efficiency value. Other possibilities, for example, chemical reactions involving TeO_3^{2-} and electrolyte species prior to ring reduction, were considered but are unlikely candidates.

Further confirmation that D1a and D2a are assignable to reactions 4 and 6, respectively, in Table I comes from controlled potential coulometry. The ratio of the anodic charge consumed in these two processes ought to be 2 if the assignments were correct; this was indeed confirmed.

The anodic current flow past D2a at the disk is assigned to the oxidation of TeO_3^{2-} to TeO_4^{2-} (reaction 7 in Table I). The sharp decrease in the ring response past R2c is consistent with previous findings that the reduction of TeO_4^{2-} to TeO_3^{2-} (or Te^{2-}) is not possible.[34] Note also that the formation of TeO_4^{2-} on the forward sweep passivates the disk surface on the return scan. The feature D1c at the disk on the return scan is assigned to the cathodic striping of Te^0 to Te_2^{2-} (reaction 5, Table I). The ditelluride ions rather than Te^{2-} (cf. reaction 4, Table I) are implicated here because of the correlated ring response R3c observed on the return scan (i.e., the direct reduction of Te^0 to Te^{2-} is expected to be kinetically sluggish). The ring response "R3c" thus is attributable to the reduction of Te_2^{2-} to Te^{2-} (reaction 3, Table I).

Figure 3 contains a cyclic voltammogram for a Cd rod in 1 M NaOH in the absence of Te^{2-} in the electrolyte. The anodic waves 1a and 2a on the forward sweep are assigned to reactions 1a and 1b in Table I, respectively. The re-

(27) Pourbaix, M. *Atlas of Electrochemical Equilibria in Aqueous Solutions*; Pergamon: New York, 1966.
(28) Park, S.-M.; Barber, M. E. *J. Electroanal. Chem.* **1979**, *99*, 67.
(29) Kröger, F. A. *J. Electrochem. Soc.* **1978**, *125*, 2028.
(30) Mishra, K. K.; Ham, D.; Rajeshwar, K., submitted for publication.
(31) Lingane, J. J.; Niedrach, L. W. *J. Am. Chem. Soc.* **1948**, *70*, 4115.
(32) Panson, A. J. *J. Phys. Chem.* **1963**, *67*, 2177.
(33) Hussain, A.; Azab, M. A.; Hassan, R. M. *Bull. Soc. Chim. Fr.* **1987**, *63*, 1.
(34) Sakashita, M.; Lochel, B.; Strehblow, H. H. *J. Electroanal. Chem.* **1982**, *140*, 75.

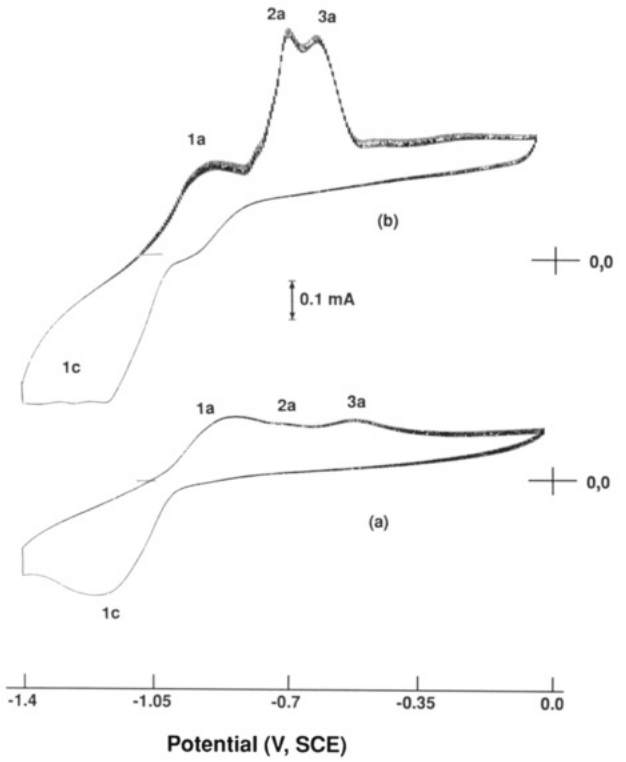

Figure 4. Cyclic photovoltammograms for a white light illuminated Cd risk in (a) 0.001 M Te^{2-} and (b) 0.1 M Te^{2-} solution in 1 M NaOH.

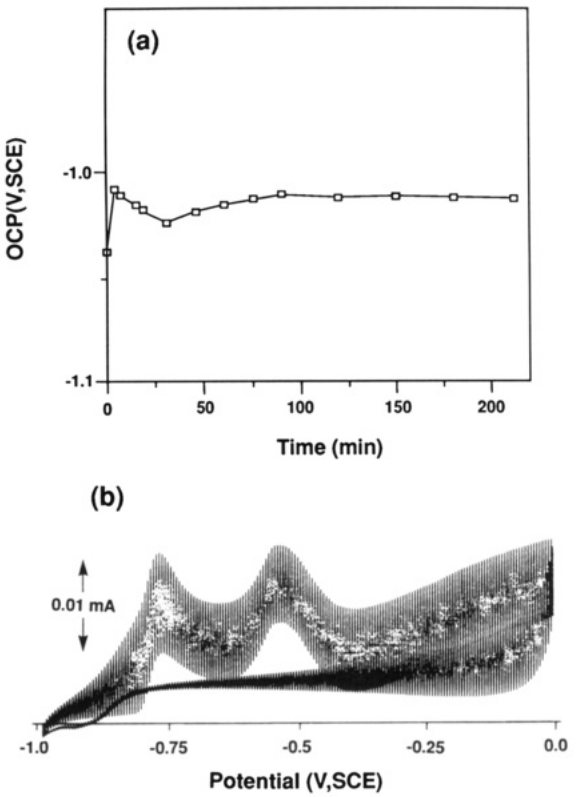

Figure 5. Photoresponse of electroless n-CdTe thin films showing the temporal evolution of an open-circuit potential of a Cd anode is 0.1 M Te^{2-}/1 M NaOH (a) and the cyclic photovoltammetry behavior in a 1 M NaOH electrolyte containing the 0.1 M Te^{2-}/Te_2^{2-} redox couple (b).

duction of these surface species generated on the forward sweep (note the *absence* of diffusion tails for both 1a and 2a in Figure 3) occurs in two steps, identified as 1c and 2c in Figure 3. These results are in general agreement with those reported by previous authors[35-37] for the Cd–H_2O system.

Cyclic photovoltammetry, unlike its "dark" counterpart, CV, has the potential of identifying the formation of photoactive species (e.g., semiconductors) on an electrode surface.[23,25,38] Figure 4 contains cyclic photovoltammograms for a Cd anode in 1 M NaOH at two Te^{2-} levels in the electrolyte. These scans were initiated in the positive-going direction at −1.40 V. Aided by the information contained in figures 2 and 3, the waves 1a, 2a, and 3a on the forward sweep are assigned to $Cd(OH)_2$ formation (reaction 1b, Table I), oxidation of Te^{2-} to Te^0 (reaction 4, Table I), and conversion of Te^0 to TeO_3^{2-} (reaction 6, Table I). The composite cathodic wave 1c in Figure 4 is assignable to the reduction of the CdTe, Cd oxides (and hydroxides), and the Te species generated on the forward sweep. Several important points with respect to the cyclic photovoltammograms in Figure 4 are worthy of note.

The modulated photoresponse seen in the CPV traces is unequivocal evidence that CdTe is indeed formed on the forward sweep. (The only other photoactive species that could possibly generate a light response is Te; however, the *photoconductivity* of this material manifests only to a very weak degee; cf. ref 23.) The observed photoresponse is *photoelectrochemical* in origin. Further, the direction of the response (photoanodic, see also Figure 5b) clearly establishes the electroformed CdTe thin film as n-type; i.e., the holes are the minority carriers and photoexcitation generates a large excess of these species; cf. ref 39. The magnitude of the photoresponse is seen to be directly proportional to the Te^{2-} concentration in the electrolyte. Note that the onset of the photoresponse is roughly coincident with the wave 1a; i.e., *the corrosion of Cd is a prerequisite to CdTe thin-film formation.* As expected, the amplitudes of the Te waves 2a and 3a also scale with the Te^{2-} concentration. We propose the following sequence for the anodic electrosynthesis of CdTe in alkaline media:

$$Cd + 2OH^- = Cd(OH)_2 + 2e^- \quad (1b)$$

$$Cd(OH)_2 + Te^{2-} = CdTe + 2OH^- \quad (15)$$

The second step differs from the more general version, reaction 10 in Table I, in that a surface place-exchange is explicitly included concomitant with Te assimilation. Note that the latter persists at potentials well past wave 3a into the "passive" regime. The photoresponse "dies" on the return sweep when potentials negative of the flatband value are accessed (i.e., the band bending at the surface then would be in the wrong direction for the collection of the photogenerated holes in the CdTe; cf. ref 39) finally culminating in the reduction wave, 1c.

A final point in the discussion of the CPV data in Figure 4 concerns the fact that the oxidation of Te^{2-} to Te^0 and that of Te^0 to TeO_3^{2-} (waves 2a and 3a, respectively) proceed on the CdTe surface. In this regard, the photogenerated holes also assist in these oxidation reactions.[39] However, there is substantial dark oxidation current flow, possibly signaling the fact that the CdTe thin film has electron-tunnelable thickness. In this regard, the uniformity of the CdTe thin-film morphology as seen in the

(35) Burstein, G. T. *J. Electrochem. Soc.* **1983**, *130*, 2133.
(36) Barnard, R. *J. Appl. Electrochem.* **1981**, *11*, 217.
(37) Birss, V. I.; Kee, L. E. *J. Electrochem. Soc.* **1986**, *133*, 2097.
(38) Mori, E.; Mishra, K. K.; Rajeshwar, K. *J. Electrochem. Soc.*, in press.
(39) Rajeshwar, K.; Singh, P.: DuBow, J. *Electrochim. Acta* **1978**, *23*, 1117.

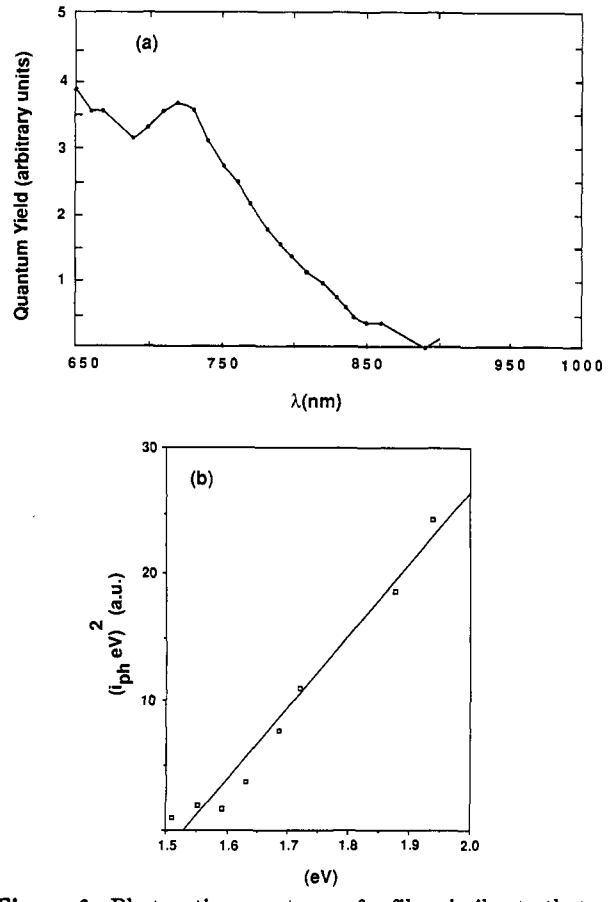

Figure 6. Photoaction spectrum of a film similar to that employed in Figure 5 with identical electrolyte composition (a) and a plot of $(i_{ph}$ (eV))^2 vs λ according to eq 16 (b).

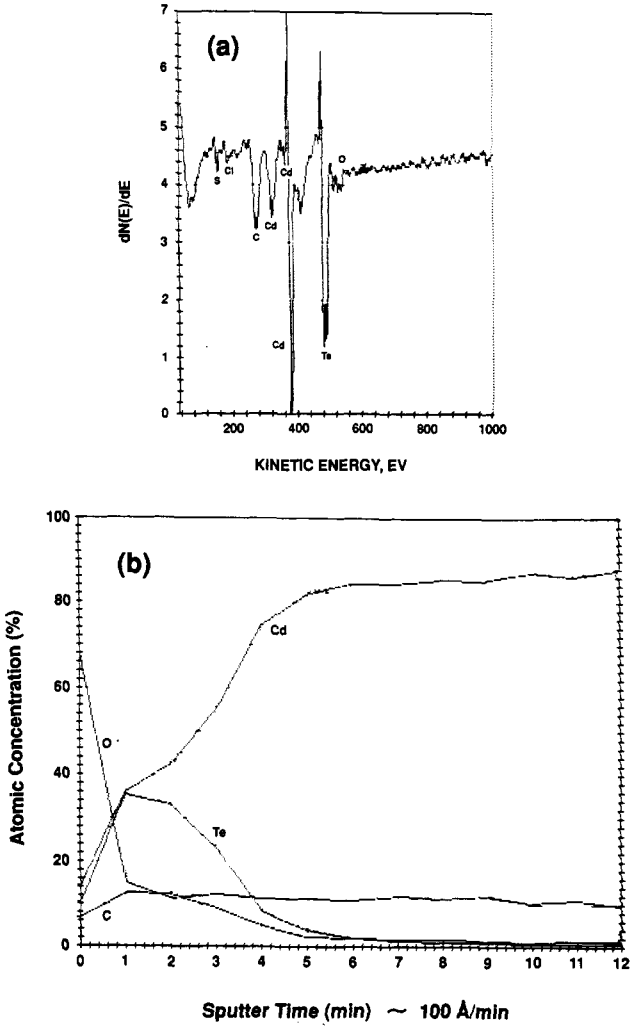

Figure 7. Auger electron spectrum in differential form for a CdTe thin film after a light Kr^+ ion etch (a) and atomic concentrations (as determined by AES) as a function of depth for a representative sample (b).

SAM data (see below) appears to render rather unlikely the possibility that direct oxidation of the Te species occurs at the exposed regions of the Cd anode surface. It is also to be emphasized that CdTe formation precedes that of Cd oxides (compare Figures 3 and 4). Further confirmation of this also comes from the surface analyses data.

How do these data compare with the behavior of other anodically electroformed semiconductor thin films? There are broad similarities with the PbS system.[19] However, unlike in the case of HgS[20] or CdS,[14-16] sharp anodic features associated with thin-film formation are absent for CdTe. The Te oxidation features at a forming CdTe surface are also unique; corresponding anodic waves for polysulfide oxidation, for example, are not seen on CdS.[14-16]

Electroless Formation of n-CdTe. Figure 5a depicts the temporal variation in the open-circuit potential of a Cd anode in 0.1 M Te^{2-} electrolyte. The potential drops over a course of 1–2 h before a steady-state value of ~−1.0 V is reached. This behavior is reminescent of corrosion/passive film formation phenomena on metal electrodes. *Note that the steady-state value lies negative of the* $Te^{2-} \rightarrow Te^0$ redox potential, *signaling that Te assimilation occurs only as CdTe* (see above). That stoichiometric CdTe thin films results (as seen, for example, by surface analyses; see below) is a logical consequence of this important point. We note that Te contamination is a general problem with the synthesis of CdTe[24] as well as other tellurides such as $Hg_{1-x}Cd_xTe$.[38]

Figure 5b contains a CV trace under chopped-light illumination for a CdTe thin film synthesized thus via the electroless route. A 0.1 M Te^{2-}/Te_2^{2-} redox electrolyte was employed in this experiment. The distinction between the scan in Figure 5b and the CPV data in Figure 4 needs to be emphasized. The latter were acquired in situ under conditions wherein a CdTe thin film was being electrosynthesized. We use the term "cyclic photovoltammetry" or CPV for this diagnostic technique.[23] On the other hand, the scan in Figure 5b is rather more conventional and has been profitably employed by previous authors[40] for the study of semiconductor electrodes.

Note that analogous to the cases in Figure 4, the photoresponse is anodic signaling that the electroless CdTe thin films are also n-type as synthesized. The CV scan in Figure 5b was initiated at −1.0 V in the positive direction. The two oxidation waves on the forward sweep correspond to the features labeled 2a and 3a in Figure 4, respectively; the corresponding wave assignments thus have already been discussed. The reduced photoactivity on the return sweep in Figure 5b is to be noted and is attributable to the passivation of the photoactive CdTe surface by the Te and Te oxides generated on the forward cycle.

Photocurrent Spectroscopy. Photoaction spectra were acquired for both types of CdTe thin films as a further diagnostic aid. Shown in Figure 6a is a representative spectrum obtained in situ for a forming CdTe thin film at open circuit. A 0.1 M Te^{2-}/Te_2^{2-} electrolyte was again employed, this time both as a Te supply and as

(40) For example: Kohl, P. A.; Bard, A. J. *J. Am. Chem. Soc.* **1977**, *99*, 7531.

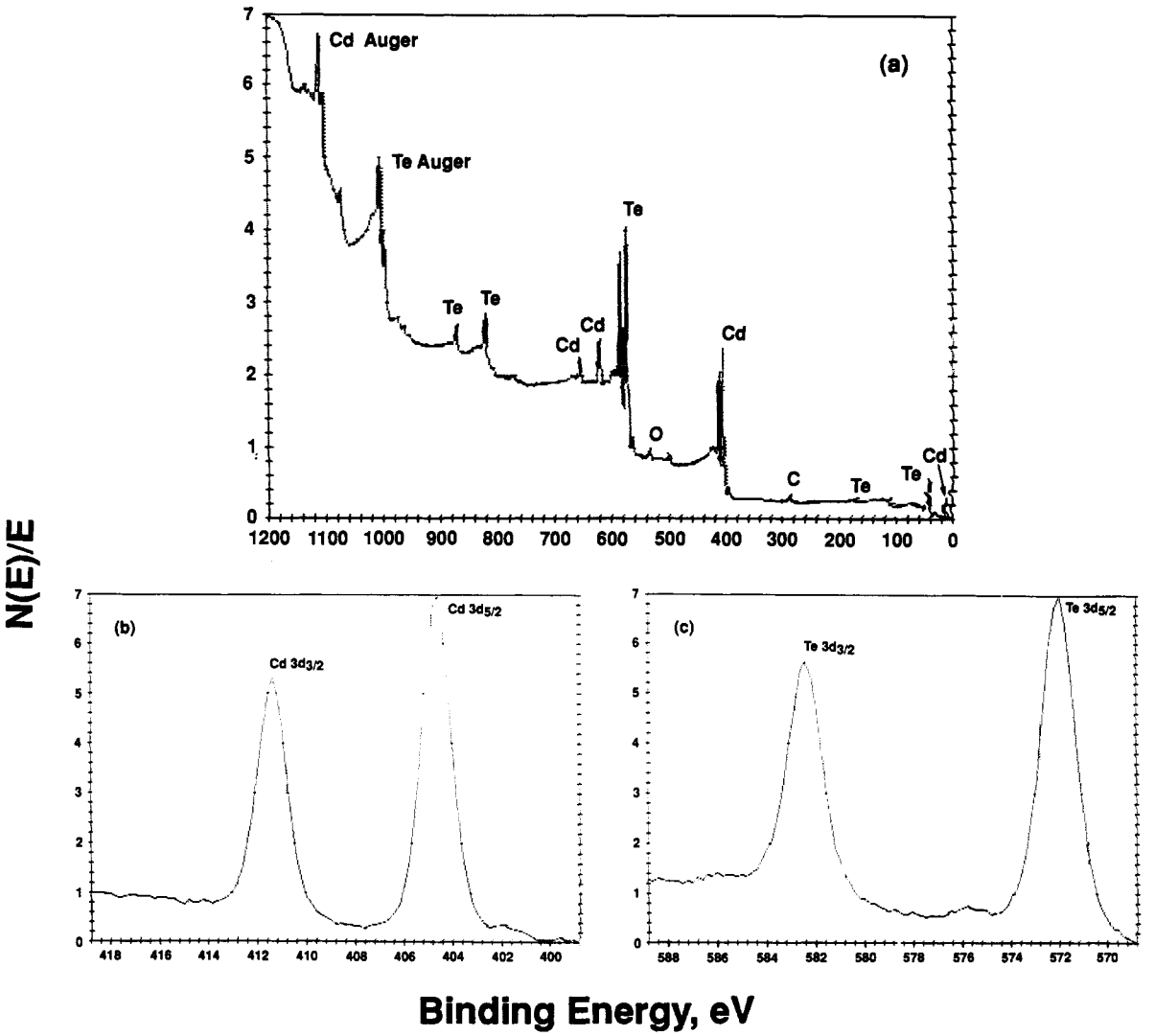

Figure 8. Survey (a) and high-resolution (b, c) XPS data for a CdTe thin film after light Kr^+ etch.

a scavenger of the photogenerated holes. A sharp decline in the photoresponse is noted at wavelengths $\geq \sim 850$ nm. Further analyses of these data were performed according to eq 16.[41] In eq 16, i_{ph} is the photocurrent, k is a constant,

$$i_{ph} = k(h\nu - E_g)^{1/2}/h\nu \qquad (16)$$

and E_g is the optical bandgap of the semiconductor. Figure 6b contains a plot of eq 16 for the data in Figure 6a; the observed intercept of ~1.5 eV is consistent with the known E_g of CdTe.

Surface Analyses. Both types of CdTe thin films i.e., samples synthesized under external potential control as well as those obtained via the electroless route, revealed similar surface compositions and morphology. Thus no distinction is made in the discussion of the surface analyses data below.

Figure 7a contains an Auger spectrum in differential form for an anodic CdTe film taken after a light krypton atom etch. the elemental concentrations determined from the Auger spectra indicated a stoichiometric ratio of Cd (27.4%) and Te (27.2%); the major impurities found were C (27.4%) and O (11.9%) with smaller amounts of S (3.0%) and Cl (2.7%). The carbon was most likely due to surface contamination, as will be discussed below. Scanning Auger maps indicated that the Te and Cd were uniformly distributed over the surface of the film. Figure 7b contains the AES depth profiling results for the same sample. These data were obtained by performing an Auger scan followed by sputtering for 1 min and then repeating this procedure until reaching the Cd (substrate) electrode. Taking the sputter rate for CdTe to be similar to ZnS (see Experimental Section) the data indicated that the cadmium concentration increased almost linearly from 35% at ~100-Å depth to 85% at ~550 Å. The Te concentration decreased from 35% at ~100 Å to 4% at ~550 Å. An oxygen-rich surface layer less than 100 Å thick was removed during the first minute of sputtering. The oxygen content then decreased linearly from 15% at ~100 Å to 4% at ~550 Å. The C level obtained from the AES depth profile was uniform at ~12% throughout the film. This indicates that the 27.4% C found in the survey scan (Figure 7a) was at the surface and removed by further sputtering.

The AES depth profiles of cathodically synthesized CdTe samples[6] differ in important respects relative to the corresonding data for the anodic specimen in Figure 7b. In the former case, approximately equal concentrations of Cd and Te were detected at the surface. However, after ~4 min of sputter time, the film was Te rich with only about half as much Cd as Te.[6] These differences are intrinsic to the differing nature of the two electrosynthesis modes. As discussed before, thermodynamic considerations render the oxidation of Te^{2-} to Te^0 less favorable than

(41) Stern, F. *Solid State Phys.* **1963**, *15*, 299.

the formation of CdTe. Thus, free Te^0 phase formation is precluded in the anodic pathway. On the other hand, in the cathodic route, *Te^0 nucleation precedes and is a requirement for CdTe formation.*[42] Thus Te^0 contamination is a common occurrence with cathodic CdTe thin-film growth.[24]

Figure 8 shows the results of a XPS survey scan (Figure 8a) and high-resolution scans for Cd (Figure 8b) and Te (Figure 8c). Integration of the high-resolution XPS peaks yielded elemental concentrations similar to those given by the Auger measurements: Cd, 31.0%; Te, 32.5%; C, 23.4%; O, 12.9%. The peak positions (charge referenced to the C 1s peak, which was taken to be 284.6 eV) indicate binding energies of 411.4 and 404.6 eV for the Cd $3d_{3/2}$ and $3d_{5/2}$ peaks and 582.4 and 572 eV for the Te $3d_{3/2}$ and the Te $3d_{5/2}$ peaks, respectively. These binding energies are within 0.1 eV of values for single-crystal CdTe reported by Kibel and Kelly[43] and are in reasonable agreement with other previously reported values.[44] Further, the peak shapes and binding energies in Figure 8c rule out the presence of significant amounts of Te oxides, which if present would have produced an easily resolved peak 3.7 eV higher in binding energy than the observed position.[43,44] Thus, we attribute the nonsurface O to the presence of $CdO/Cd(OH)_2$ in minor quantities in addition to CdTe as the major component.

In conclusion, we have demonstrated that CdTe thin films with little contamination from Te^0 may be electrosynthesized via an anodic route. A anodic electroless technique was also used for the first time to electrosynthesize n-type CdTe thin films.

Acknowledgment. We thank the National Science Foundation (Grant MSM 86-17850) for partial financial support of this research. It is also a pleasure to acknowledge the support of the Research Enhancement Program of The University of Texas at Arlington. A.W. additionally thanks the Robert A. Welch Foundation and the Texas Advanced Research Program for funding support. M. Murley of LTV, Dallas, TX, provided the surface analysis data.

Registry No. CdTe, 1306-25-8; Cd, 7440-43-9; Na_2Te, 12034-41-2; Te^{2-}, 22541-49-7; Te_2^{2-}, 62086-49-1; Kr, 7439-90-9.

(42) Mori, E.; Rajeshwar, K. *J. Electroanal. Chem.* **1989**, *258*, 415.
(43) Kibel, M. H.; Kelly, C. G. *Mater. Australasia* **1987**, *Nov/Dec*, 15.
(44) Briggs, D.; Seah, M. P. *Practical Surface Analysis*; Wiley: Chichester, UK, 1982.

A Surface Characterization and Depth Profiling Study of Conventional Electrodeposited Chromium Films. 3

Gar B. Hoflund,* Mark R. Davidson, and Eva Yngvadottir

Department of Chemical Engineering, University of Florida, Gainesville, Florida 32611

Herbert A. Laitinen

Department of Chemistry, University of Florida, Gainesville, Florida 32611

Shigeo Hoshino

Musashi Institute of Technology, 1-28, Tamazutsumi, Setagaya-ku, Tokyo 158, Japan

Received April 20, 1989

In this study the composition and chemical interactions of chromium layers produced in a conventional Sargent bath have been examined using Auger electron spectroscopy (AES), electron spectroscopy for chemical analysis (ESCA), ion scattering spectroscopy (ISS), and depth profiling before and after annealing the sample in air or vacuum. Future comparisons between these results and similar results obtained from chromium layers prepared by the amorphous bright chromium deposition (ABCD) method (Hoshino, S.; Laitinen, H. A.; Hoflund, G. B. *J. Electrochem. Soc.* **1986**, *133*, 681) should be useful in understanding why the ABCD films behave differently than conventional Cr films. ABCD films have many desirable properties compared to deposits produced by conventional methods. Most importantly, the hardness of ABCD films increases with annealing temperature up to 700 °C, whereas the hardness of conventional chromium films decreases. The results of this study indicate that S, C, Cl, O, Ca, K, and Na are incorporated into the conventional chromium films from the electrolytic bath. Cr is present as a sulfide, metal, and oxides. Annealing the sample in air or vacuum (10^{-4} Torr) causes sulfur to desorb from the surface probably as SO_2. Annealing the sample in high vacuum (5×10^{-9} Torr) causes sulfur to segregate to the surface and remain there while oxygen migrates to the surface and desorbs. This results in conversion of the surface chromium oxides into Cr_2S_3 and metallic Cr. Carbon present in the background gas during annealing is adsorbed and incorporated into the bulk of the film.

Introduction

Chromium plating is widely used in the manufacture of machines and instruments in the automobile and other industries to improve the wear resistance of metallic surfaces and protect them against corrosion. Sargent[1] and Fink[2] developed and described methods that use chromic acid solutions containing a sulfate catalyst for chromium plating. The chromium plating layers formed by this method have many defects, which may be described as crack and pinhole defects. Also, the hardness of these

(1) Sargent, G. J. *Trans. Am. Electrochem. Soc.* **1920**, *37*, 479.
(2) Fink, C. G. U.S. Patent 1,581,188, 1926.

0897-4756/89/2801-0625$01.50/0